

DESIGN AND EXPERIMENTAL OPTIMIZATION OF V-SHAPED HAMMER FOR HAMMER MILL

锤片式粉碎机 V 型锤片设计及试验优化

Haijun ZHANG^{1,2)}, Yi QIAN²⁾, Haiqing TIAN²⁾

¹⁾ Huzhou Vocational and Technical College, Intelligent Manufacturing and Elevator College, Huzhou / China;

²⁾ Inner Mongolia Agricultural University, College of Mechanical and Electrical Engineering, Hohhot / China

Tel: +086-0572-2363665; E-mail: zhanghj320@163.com

DOI: <https://doi.org/10.35633/inmateh-73-16>

Keywords: Hammer mill, Feed, Grinding, V-shaped hammer, Parameter optimization, Orthogonal tests, ANSYS analysis

ABSTRACT

Low productivity and high electricity consumption are considered problems of the hammer mill, which is widely used in current feed production. In this paper, a folded V-shaped hammer was designed to improve the performance of the hammer mill. To determine the optimal design parameters of the new hammer, the single-factor test and orthogonal tests were carried out with the inclination angle of hammer, the angle of hammer head, and the distance of hammer head as the influencing factors, and the productivity and output per kWh as evaluation indexes. The order of the influence on the productivity and output per kWh were the inclination angle of hammer > the angle of hammer head > the distance of hammer head. The parameters were optimized based on the orthogonal tests with the following results: the angle of hammer head was 160°, inclination angle of hammer was 110°, and the inclination distance of hammer head was 24 mm. The static analysis and modal analysis were carried out on the optimized hammer by using ANSYS software. The results showed that the new hammer satisfies the strength and stiffness requirements during working, does not resonate, and has good dynamic characteristics. The new hammer can effectively improve the performance of the hammer mill, and the research results can provide theoretical basis for the optimization design of the hammer mill.

摘要

针对目前生产中普遍使用的锤片式粉碎机存在生产率低、能耗高的问题。本文以 CPS-420 型锤片式粉碎机为研究样机，对锤片式粉碎机物料粉碎过程和物料力学特性进行分析，设计了折线式 V 型锤片，提高粉碎机性能。为确定锤片最佳设计参数，以锤片倾角、锤头角度和倾角距离为因素，以生产率和度电产量为评价指标，开展了单因素试验和正交试验，结果表明：影响生产率和度电产量的因素主次顺序均为锤头角度 > 锤片倾角 > 倾角距离。基于正交试验进行参数优化，优化结果为：锤头角度为 160°、锤片倾角为 110° 和倾角距离为 24 mm。对优化后的锤片进行静力学分析和模态分析，结果表明：锤片满足工作时的强度和刚度要求，不会发生共振，有较好的动态特性。新型锤片能有效提高锤片式粉碎机的性能，研究结果可为锤片式饲料粉碎机的优化设计提供理论依据。

INTRODUCTION

Feed grinding can increase the surface area of feed and improve its palatability and digestibility for livestock. Therefore, a large amount of feed needs to be ground every year (Mugabi et al., 2017; Wang et al., 2020; Barnwal et al., 2015). The hammer mill is a widely used grinding equipment in feed processing, and it has the advantages of low price, simple structure and easy operation (Chen et al., 2017; Qian, 2021). However, there are still some problems, such as low productivity and high electricity consumption with the hammer mill (Li et al., 2019; Cao et al., 2016; Wang et al., 2020).

The material is ground by the hammer in the grinding chamber. The hammer is key part that affect the productivity and electricity consumption of the hammer mill (Li et al., 2019; Qian, 2021). In recent years, researches on the hammer of the hammer mill in China and abroad have mainly focused on the arrangement, manufacturing process and numbers of the hammer, etc.

Xu Wei *et al.*, (2021), took the minimum deformation of the traditional hammer as the optimization objective and used the response surface method and genetic algorithm to optimize the structure parameters of the hammer. Bochat *et al.*, (2015), designed a new hammer and performed comparative experiments. The results showed that the new hammer was more efficient than the traditional hammer. Su Congyi *et al.*, (2016), designed a new hammer and performed comparative experiments. The results showed that the new hammer reduced the centrifugal inertia force of the material and the density of the material ring, the efficiency of the hammer mill was improved by 25% to 28%. Ma Qian *et al.*, (2016), studied the influence of the hammer inclination angle on the grinding performance by using computational fluid dynamics methods. Simulation results showed that the hammer with an inclination angle could improve the flow field characteristics of the grinding chamber and the efficiency of the hammer mill. CPS-420 hammer mill was taken as the experimental prototype, Li Xiuqing, (2021), designed an edged hammer and an angled hammer, discrete element simulation and grinding performance tests were carried out. The results showed that both the edged hammer and the angled hammer could improve the grinding performance. The angled hammer could change the flight trajectory of materials, reduce movement speed of materials, and the angled hammer was beneficial to sieve. The hammer mill with an inclined hammer was beneficial for reducing electricity consumption. The edged hammer could break more material bonding keys, improve the production efficiency of the hammer mill.

In this work, a hammer mill CPS-420 produced by machinery factory of Inner Mongolia Agricultural University in China was taken as the prototype. Considering the existing problems with the hammer mill, the grinding process of materials in the grinding chamber was analysed, a folded V-shaped hammer was designed to improve the performance of the hammer mill, and the key structural parameters of the new hammer affecting the performance of the hammer mill were determined. The orthogonal tests were used to optimize the structural parameters of the hammer, and the optimal combined parameters were determined. The research results can provide a reference for the optimal design of the hammer mill.

MATERIALS AND METHODS

• Overall structure and working principle

The hammer mill used in this study is mainly composed of an outlet, a frame, a motor, a feeding hopper, a sieve, and a hammer. The structure diagram of the hammer mill is shown in Figure 1. When the hammer mill is working, the feed materials enter the grinding chamber through the feeding hopper. It is first ground by the hammer and then further ground by the impact between the feed and sieve. When the feed particle size is smaller than the sieve hole diameter, the feed is discharged from the outlet.

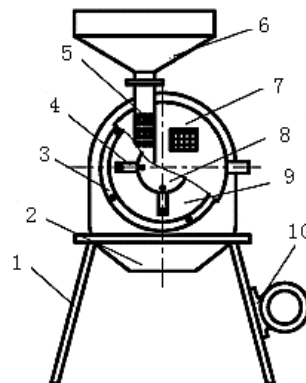


Fig. 1 - Structure diagram of the hammer mill

1-Frame; 2-Outlet; 3-Sieve frame and sieve; 4-Hammer; 5-Air inlet of feeding mouth; 6-Feeding hopper; 7-Cover plate of grinding chamber; 8-Hammer frame; 9-Grinding chamber; 10-Motor

Table 1

Specification of hammer mill	
Specification	Value
Size (Length×Width×Height)	650×380×930 mm
Motor power	3 kW
Rotational speed of rotor	4 400 r/min
Number of hammers	24
Sieve width	170 mm
sieve hole diameter	3 mm
Productivity	900~950 kg/h

● **Principle analysis of material grinding**

When the hammer mill is working, the materials in the grinding chamber are mainly ground by the combined action of the hammer, the sieve, and material particles. The schematic diagram of movement of material particles in the grinding chamber is shown in Figure 2. The linear speed of the hammer is v . Assuming that the impact between the hammer and the material is a frontal impact, the speed of the material after the impact is v_1 , which is the same as v . Energy transfer is completed at the moment of impact, the kinetic energy of the high-speed rotating hammer is transferred to the material particles. After impact, the material particles move in the direction of v_1 and impact with the sieve in the grinding chamber. The kinetic energy of the material particles decreases, and the lost energy during the impact process is used to destroy the cohesive force of the material particles themselves, causing the material to quickly grind.

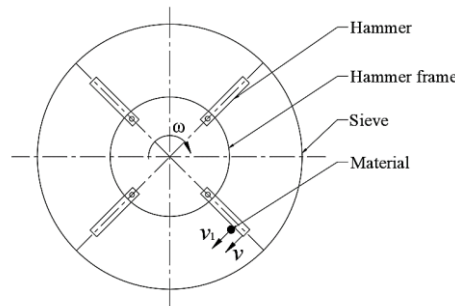


Fig. 2 - Schematic diagram of movement of material particles

● **Design of V-shaped hammer for the hammer mill**

According to Figure 2, the material particles enter the grinding chamber from the feeding hopper and mainly impact with the side surface of the hammer end. Without considering the influence of factors such as air flow resistance and friction on the hammer, the following equation can be obtained from the impulse momentum theorem (Qian, 2021).

$$P\Delta t = m_1(v - v_2) \tag{1}$$

where: P is the impact force between the hammer and the material, N; m_1 is the mass of hammer, kg; Δt is the impact time between hammer and material, s; v is the speed of the hammer before impact, m/s; v_2 is the speed of the hammer after impact, m/s.

According to Eq. (1), if the speed of hammer and the speed of material are constant, the impact of the hammer on the material is increased with the increases of m_1 , accelerating the grinding efficiency of large particle materials into small particles, thereby improving the grinding performance of the hammer mill.

In addition, it found that the impact angle of particles thrown onto the sieve after being impacted by the hammer affects the sieving effect of the material. The impact of the hammer on the material particles in the grinding chamber is shown in Figure 3.

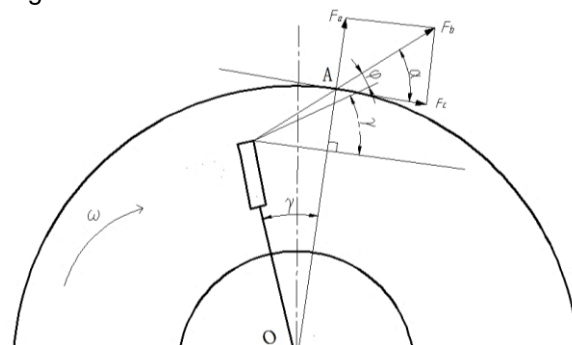


Fig. 3 - Schematic diagram of material particles impacting screen plate

It can be seen from Figure 3 that after the traditional hammer impacts with material particles, its ejection angle is φ , point A is the impact point between the material and the sieve, α is the impact angle, γ is the angle between the centre line of the hammer and the radial centre line of point A on the sieve, F_b is the combined force of the material particles under the impact of the hammer, F_a and F_c are the positive and side impact force, they are the two components of F_b . The following equations can be obtained (Du, 2015):

$$\alpha = \varphi + \gamma \tag{2}$$

$$F_a = F_b \sin \alpha \tag{3}$$

An analysis of Eq. (2) and Eq. (3) show that the larger the impact angle, the greater the positive impact force, which is more conducive to the grinding and sieving effect of the material. The optimized hammer should increase the impact angle of the material on the sieve, so that the ground material can be quickly sieved out and achieve efficient grinding of the material.

During the working process of the hammer mill, the material is mainly ground by the impact between the end of the hammer and the material. Based on the above theory and referring to the picking mechanism of the straw baler (Qian, 2021), a new design scheme of a folded hammer structure was proposed. The end of the hammer was designed as a V-shaped structure with a fold line, which can improve the quality of the hammer appropriately. On the other hand, it increases the impact probability between the hammer and the material, thereby improving the grinding efficiency of the hammer mill. The schematic diagram and physical picture of the new hammer structure are shown in Figure 4.



Fig. 4 - Parameters of V-shaped hammer

Note: In Fig.4a: a- Inclination angle of hammer; b-Angle of hammer head; c-Inclination distance of hammer head

• Design of hammer thickness

The overall thickness of the hammer has a significant impact on the grinding performance of the hammer mill. If the hammer is too thin, it will cause its wear resistance to deteriorate and require frequent replacement, which not only increases the labour intensity of maintenance workers but also increases the cost of material grinding. The hammer is too thick, although it increases the probability of the material being hit, the load on the rotor of the hammer mill will increase, resulting in huge electricity consumption.

Therefore, based on the structural parameters of the grinding chamber of the CPS-420 hammer mill, the thickness of the hammer was designed by the following equation:

$$Z = K_2 B / \delta \quad (4)$$

where: Z is the thickness of hammer; K_2 is the density coefficient of hammer configuration. Generally, K_2 is taken as 0.2~0.42; B is the width of grinding chamber, $B=170$ mm; δ is the total count of hammer, $\delta=24$.

Based on the analysis of the density of the prototype hammer in this study, it was found that K_2 is 0.42. According to Eq. (4), the thickness of the new hammer was calculated to be 2.98 mm, for processing convenience, Z was taken as 3 mm.

In addition, the effective impact area between the traditional rectangular hammer of the hammer mill and the material is determined by the following equation:

$$S_1 = B_1 \times P_1 \quad (5)$$

where: S_1 is the effective impact area of the traditional hammer, mm^2 ; B_1 is the thickness of the traditional hammer, mm; P_1 is the length of the traditional hammer, mm.

Bringing B_1 and P_1 into Eq. (5), it can be obtained $S_1 = 2.5 \times 101 = 252.5(\text{mm}^2)$.

The optimized hammer end is a double-sided structure, and the effective impact area of the hammer is:

$$S_2 = B_2 \times (P_2 + P_3) \quad (6)$$

where: S_2 is the effective impact area of the optimized hammer, mm^2 ; B_2 is the thickness of the optimized hammer, mm; P_2 and P_3 are the lengths of the optimized hammer and its head, respectively, mm.

Bringing B_2 , P_2 and P_3 into Eq. (6), it can be obtained $S_2 = 3 \times (105 + 11) = 348(\text{mm}^2)$

According to the analysis of Eq. (5) and Eq. (6), it can be seen that the effective impact area of the optimized hammer is about 1.4 times greater than that of the traditional hammer, thereby increasing the probability of impact between the material and the hammer.

• Design of hammer length

The length of the hammer affects the gap between the hammer and sieve. When the hammer mill is working, there is a material circulation layer between the end of the hammer and the sieve that rotates with the hammer. When the distance between the end of the hammer and the sieve is too large, the small particle materials have been ground near the end of the hammer are not easy to be sieved out. If the distance is too small, the velocity of the circulation layer increases, the particle size of the material is low, and it increases the electricity consumption.

It was found that the distance between the end of the hammer and the sieve is generally between 7 mm to 10 mm (Qian *et al.*, 2020). In this paper, the distance is 9 mm.

The length of the hammer is determined by the following equation:

$$r_1 = R_1 - \Delta R - L_i \quad (7)$$

where: r_1 is the distance from the centre of the pin shaft installation hole to the end of the hammer, mm; R_1 is the radius of the sieve, $R_1=195$ mm; ΔR is the distance between the end of the hammer and the sieve, $\Delta R = 9$ mm; L_i is the distance from the centre of the rotor to the centre of the pin shaft installation hole, $L_i=92$ mm.

Bringing R_1 , ΔR and L_i into Eq. (7), it can be obtained $r_1 = 94$ mm.

● Parameter design of hammer experiment

The design of the new hammer structure of the hammer mill should not only satisfy the hammer installation size, but also consider the distance between the end of the hammer and the sieve. The angle of hammer head of the new hammer directly affects the grinding characteristics of the hammer. Considering the motion characteristics of the ground material in the grinding chamber and the structural parameters of the hammer mill, the ranges of hammer head were set to 90° to 150° ; considering the wear angle and position of the end of the hammer, the inclination distances of hammer head were set to 15 mm to 30 mm. In addition, the circulation area between the end of the hammer and the sieve in the grinding chamber has a significant impact on the sieving and grinding of the material. The airflow characteristics in the circulation area are closely related to the inclination angle of hammer. According to Qian *et al.*, (2021), it was found that when the inclination angle of hammer changes from 140° to 165° , the material can achieve better sieving performance. Therefore, the inclination angles of hammer were set to 140° to 165° .

● Experimental design

In order to study the influence of the structural parameters of the new hammer on the grinding performance of the hammer mill, and determine the optimal hammer structure parameters. The experiment of grinding performance was carried out based on the inclination angle of hammer, the angle of hammer head, and the inclination distance of hammer head.

● Experimental materials and equipment

Corn grain was selected as the test material. The average moisture content of corn grain was 13.2%. The variety of corn used was JINSHAN-126, with a moisture content of 13.20% and bulk density of 723 kg/m^3 . The test equipment included a TCS-150 type electronic scale (accuracy of 0.01 kg), a BT223S type electronic balance (accuracy of 0.001 g), an electric energy meter, a stopwatch and a drying box, etc.

● Evaluation indexes

In order to objectively and accurately evaluate the grinding performance of the hammer mill, according to the Chinese national standard (GB/T 6971-2007) (China National Standardization Committee, 2007), the productivity and electricity consumption per ton were taken as the performance evaluation indexes.

The calculation equations are given by Eq. (8) and Eq. (9) (China National Standardization Committee, 2007).

$$E = m/t_c \quad (8)$$

$$Y = Z/Q \quad (9)$$

where:

E is the productivity, t/h; m is the material mass, t; t_c is the material grinding time, h.

Y is the output per kWh, t/kWh; Q is the electricity consumption, kWh; Z is the output, t.

● Test procedures

The new hammers with different structural parameters were installed on the hammer mill to carry out the grinding performance tests. The test procedures were as follows:

(1) The hammer mill ran no-load firstly, and after the no-load power stabilizes, the spindle speed was measured to verify whether the speed meets the requirements of the hammer mill.

(2) The hammer mill ran with load, and it ran smoothly for 1 to 2 minutes, after confirming that there are no abnormal phenomena, the grinding performance test was carried out according to the test scheme.

(3) In order to increase the accuracy of experimental data, each group of tests was repeated three times. The average values were taken as the test results.

RESULTS

- **Single-factor test results and analysis**

- Results and analysis of the inclination angle of hammer*

The values 140°, 145°, 150°, 155°, 160°, and 165° were selected as the inclination angle of hammer, productivity and output per kW·h tests were carried out. The test results are shown in Table 2.

Table 2

Inclination angle of hammer	Productivity	Output per kWh
[°]	[t/h]	[t/kWh]
140	0.89	5.12
145	0.94	4.93
150	1.02	4.80
155	1.07	4.72
160	0.98	4.82
165	0.92	5.13

It can be seen from Table 2 that with the inclination angle of hammer increases, the productivity first increases and then decreases, and the output per kWh first decreases and then increases. When the inclination angles of hammer were 155°, the productivity was highest and the output per kWh per ton of material was lowest; from the trend of changes in productivity and output per kWh, it can be seen that the better inclination angle ranges of the hammer were 150° to 160°.

- Results and analysis of the angle of hammer head*

90°, 100°, 110°, 120°, 130°, and 140° were selected as the angle of hammer head, productivity and output per kW·h tests were carried out. The test results are shown in Table 3.

Table 3

Angle of hammer head	Productivity	Output per kWh
[°]	[t/h]	[t/kWh]
90	0.96	5.03
100	0.99	4.87
110	1.04	4.82
120	1.02	4.90
130	0.93	5.12
140	0.89	5.08

It can be seen from Table 3 that with the angle of hammer head increases, the productivity first increases and then decreases, the output per kWh shows a waveform trend. When the angle of hammer head was 110°, the productivity was highest and the output per kWh was lowest. From the trend of changes in productivity and output per kWh, it can be seen that the better angles of hammer head were 100° to 120°.

- Results and analysis of the inclination distance of hammer head*

The values 15 mm, 18 mm, 21 mm, 24 mm, 27 mm and 30 mm were selected as the inclination distance of hammer head, productivity and output per kWh per ton of material tests were carried out.

The test results are shown in Table 4.

Table 4

Inclination distance of hammer head	Productivity	Output per kWh
[mm]	[t/h]	[t/kWh]
15	0.97	5.01
18	0.90	4.92
21	0.95	4.83
24	1.03	4.84
27	1.01	4.81
30	0.98	4.92

It can be seen from Table 4 that with the inclination distance of hammer head increases, the productivity first decreases and then increases, and then decreases again.

The output per kWh first increases and then decreases. When the inclination distance of hammer head was 24 mm, the productivity was the highest; when the inclination distance of hammer head was 27 mm, the output per kWh was the lowest; from the trend of changes in productivity and output per kWh, it can be seen that the better inclination distances of hammer head were 24 mm to 30 mm.

- **Orthogonal tests results and analysis**

In order to obtain the optimal working parameters combination of the hammer, three-factor, and three level orthogonal tests were carried out. According to the single-factor test results, the level of each factor was determined as shown in Table 5.

Table 5

Level of factor	Inclination angle of hammer	Angle of hammer head	Inclination distance of hammer head
	A	B	C
	[°]	[°]	[mm]
1	150	100	24
2	155	110	27
3	160	120	30

The results of the orthogonal tests are shown in Table 6. It can be seen from Table 6 that the range of factor B in productivity test and output per kWh test was 0.1 and 0.2 respectively, both of which were the maximum values, indicating that the factor B had the greatest impact on productivity and output per kWh. The range of factor A was 0.06 and 0.08 respectively, both of which were greater than factor C, indicating that the factor A had a secondary impact on the productivity and output per kWh; The range of factor C was 0.05 and 0.06 respectively, both of which were the smallest, indicating that the factor C had the smallest impact on productivity and output per kWh. Using the range analysis method, the rankings of the three factors according to the importance to the productivity and output per kWh were obtained, successively, they were factor B > factor A > factor C. The combined optimal parameters of productivity were as follows: B₂A₁C₁. The combined optimal parameters of output per kWh were as follows: B₂A₃C₁.

The B₂ level of factor B was selected twice, so B₂ was the optimal level for factor B. The C₁ level of factor C was selected twice, so C₁ was the optimal level for factor C. The A₃ level and A₁ level of factor A were selected once each, therefore, the optimal level of factor A was between A₃ and A₁. It can be seen from Table 6 that the E_{k1} plus Y_{k1} was less than E_{k3} plus Y_{k3}, so the A₃ was the optimal level for factor A. The final combined optimal parameters were as follows: B₂A₃C₁.

Table 6

Factor test number	Inclination angle of hammer	Angle of hammer head	Inclination distance of hammer head	Empty column D	Productivity E	Output per kW·h Y
	A	B	C			
	[°]	[°]	[mm]	\	[t/h]	[t/kWh]
1	1	1	1	1	0.97	4.84
2	1	2	2	2	1.03	4.87
3	1	3	3	3	0.98	4.86
4	2	1	2	3	0.92	4.97
5	2	2	3	1	0.96	5.04
6	2	3	1	2	0.93	4.81
7	3	1	3	2	0.87	4.78
8	3	2	1	3	1.08	5.20
9	3	3	2	1	0.94	4.85
E _{k1}	0.99	0.92	0.99	0.96		
E _{k2}	0.93	1.02	0.96	0.94		
E _{k3}	0.96	0.95	0.94	0.99		
E _{Range R}	0.06	0.1	0.05	0.03		
E Importance ranking affected by the three factors					B>A>C	
E Optimal parameter					B ₂ A ₁ C ₁	
Y _{k1}	4.86	4.86	4.95	4.91		
Y _{k2}	4.9	5.04	4.90	4.82		
Y _{k3}	4.94	4.84	4.89	5.01		
Y _{Range R}	0.08	0.2	0.06	1.78		
Y Importance ranking affected by the three factors					B>A>C	
Y Optimal parameter					B ₂ A ₃ C ₁	

Note: E_{k1}, E_{k2}, and E_{k3} represented the average value of the sum of the three evaluation indicators of productivity for the same parameter at the same level, t/h; Y_{k1}, Y_{k2}, and Y_{k3} represented the average value of the sum of the three evaluation indicators of output per kW·h for the same parameter at the same level, t/kWh.

- **Static results and analysis of the hammer**

The hammer is the key component of the hammer mill. Static analysis of the optimized hammer will be carried out, which can identify dangerous cross-sectional areas in the design, and improve the shortcomings in the design. In this work, static analysis on the optimized hammer was carried out by ANSYS software. The mesh is shown in Figure 5.

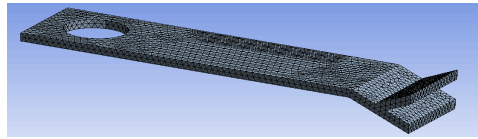


Fig. 5 - Hammer mesh

Due to the high-speed rotation of the hammer in the grinding chamber, compared to the unloaded situation, the load on the hammer under loading is relatively large, so only the loading situation was analysed and calculated.

According to the momentum theorem, the impact force between the material and the hammer is as follows:

$$P\Delta t_1 = m_1\Delta v \quad (10)$$

where: Δt_1 is the contact time between the material and the hammer, s; Δv is the variable of velocity of hammer after contact with the material, m/s; m_1 is the mass of hammer, kg; P is the impact force between the material and the hammer, N .

Bringing Δt_1 , m_1 and Δv into Eq.(10), it can be obtained $P = \frac{0.00493 \times (85.2 - 45.6)}{0.001} = 195.2(N)$.

The impact force, the rated speed, the constraints, etc. of the material and hammer were added to the hammer, and the static calculation and solution on the hammer were carried out. The equivalent stress cloud map and deformation cloud map of the hammer are shown in Figure 6.

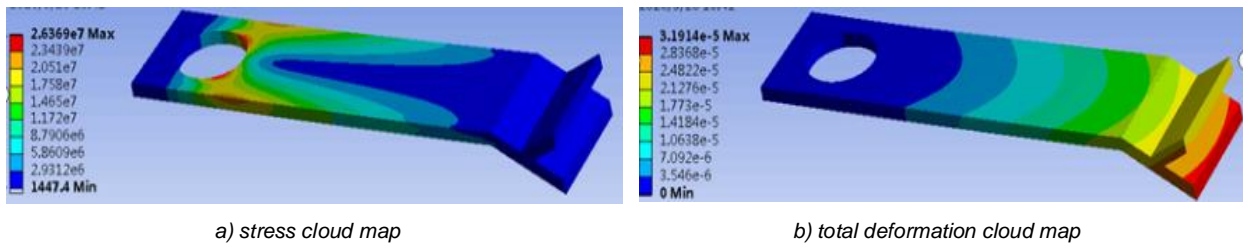


Fig. 6 - Static analysis simulation cloud chart of new hammer

It can be seen from Figure 6a that the stress of the hammer was mainly concentrated at the circular hole that matched with the pin shaft, the stress variation range was 0.0145 MPa to 26.37 MPa. The stress of the hammer was mainly between 0.01445 MPa to 14.7 MPa. The material of the hammer was 45# steel, its yield strength was 355 MPa, which was much greater than the maximum stress of the hammer. From the stress analysis, the hammer satisfies the strength and stiffness requirements during working.

It can be seen from Figure 6b that the maximum deformation in the X direction was 7.41 μm . The maximum deformation in the Y direction was 4.35 μm . The maximum deformation in the Z direction was 7.42 μm . The total deformation was 31.9 μm . Therefore, the deformation of the hammer was very small, and there will be no structural damage during working.

- **Modal results and analysis of the hammer**

Objects with different structures have different natural frequencies. When the external excitation frequency is consistent with the natural frequency, the object will resonate. Therefore, modal analysis of key components is crucial. Modal results of the new hammer are shown in Figure 7. According to the working principle of the hammer, the maximum excitation frequency of the hammer during working is the excitation frequency generated by the rotor rotating at the rated speed. The maximum speed of the rotor was 4400 r/min, so the maximum excitation frequency of the hammer was 73.33 Hz. The first-order to sixth order natural frequencies of the hammer were 7.556 Hz, 8.377 Hz, 9.563 Hz, 10.450 Hz, 11.880 Hz and 11.109 Hz, respectively, the maximum excitation frequency of the hammer was much greater than the natural frequency. Therefore, resonance was effectively avoided and the dynamic characteristics are good.

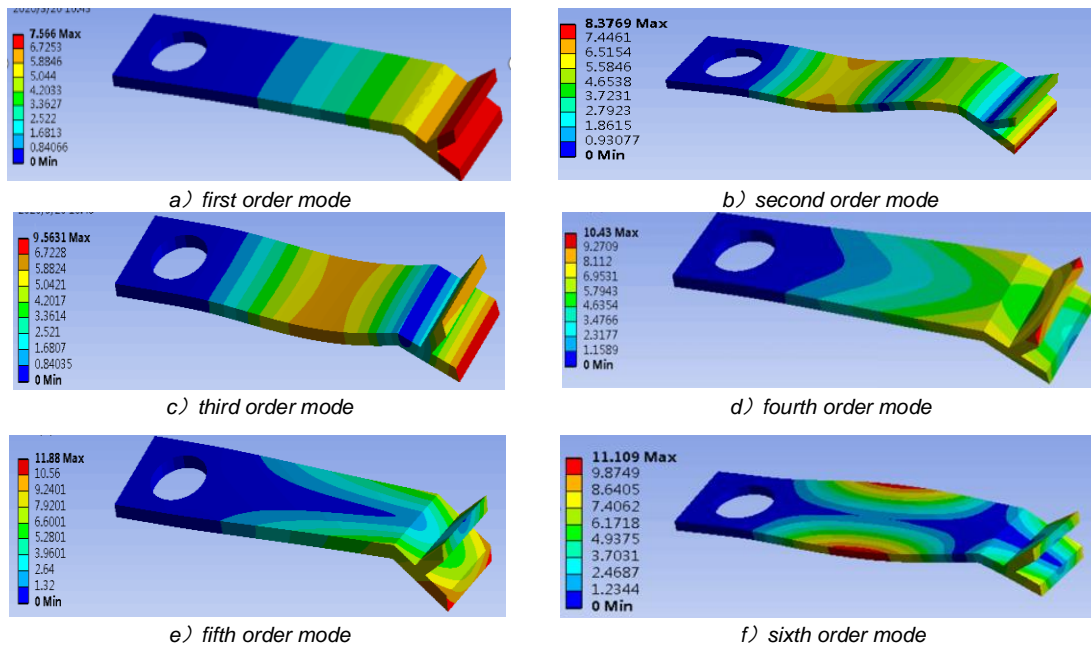


Fig. 7 - Modal results and analysis of the new hammer

The previous studies mainly focused on the structure of the hammer mill and the shape of the grinding chamber, with the goal of improving the efficiency and reducing energy consumption of the hammer mill, a series of studies were carried out. Hammer is a key component for crushing materials, some scholars have studied the material and wear resistance of hammer, but have not studied the structure and shape of hammer. Therefore, this article focuses on optimizing the design of hammer, a folded V-shaped hammer was designed. The hammer mill installed the V-shaped hammer, which not only improved production efficiency but also reduced energy consumption. The research results can provide theoretical basis for the optimization design of the hammer mill.

CONCLUSIONS

1. Taking the hammer of CPS-420 hammer mill as the studied object, the grinding process of materials in the grinding chamber was analysed. It was found that changing the shape of the hammer reasonably could increase the probability of material being hit. Combined with the dynamic characteristics of material grinding, a design scheme of a folded V-shaped hammer was proposed, the folded V-shaped hammer effectively increased the contact area with the material, thereby it effectively improved the grinding performance of the hammer mill.

2. Taking the inclination angle of hammer, the angle of hammer head, and the inclination distance of hammer head as the influencing factors, and the productivity and output per kWh as evaluation indexes, the grinding performance of the hammer mill was experimentally studied through single factor test and orthogonal tests. The results of the single factor test showed that the optimal parameter range for the inclination angle of hammer was 150° to 160° , the optimal parameter range for the angle of hammer head was 100° to 120° , and the optimal parameter range for the inclination distance of hammer head was 24 mm to 30 mm. The orthogonal tests results showed that the rankings of the three factors according to the importance to the productivity and output per kWh were obtained, successively, they were the angle of hammer head, the inclination angle of hammer and the inclination distance of hammer head. The final combined optimal parameters of the hammer are as follows: 160° the angle of hammer head, 110° the inclination angle of hammer and 24 mm the inclination distance of hammer head.

3. The static analysis and modal analysis were carried out on the optimized hammer by using ANSYS software. The static analysis results showed that the stress variation range of the new hammer was 0.0145 MPa to 26.37 MPa. The stress of the hammer was mainly concentrated at the circular hole that matched with the pin shaft. The total deformation was $31.9 \mu\text{m}$, the hammer satisfies the strength and stiffness requirements during working. The modal analysis results showed that the first-order to sixth order natural frequencies of the hammer were 7.556 Hz, 8.377 Hz, 9.563 Hz, 10.450 Hz, 11.880 Hz and 11.109 Hz, respectively, the maximum excitation frequency of the hammer was 73.33 Hz, which was much greater than the natural frequency, resonance was effectively avoided and the dynamic characteristics were good.

ACKNOWLEDGEMENT

This research was funded by the National Natural Science Foundation of China (51765055)

REFERENCES

- [1] Barnwal, P., Singh, K. K., Sharma, A. et al. (2015). Influence of pin and hammer mill on grinding characteristics, thermal and antioxidant properties of coriander powder. *Journal of Food Science and Technology*, 52(12), 7783-7794. <https://doi.org/10.1007/s13197-015-1975-0>
- [2] Bochat, A., Wesolowski, L., Zastempowski, M. (2015). A comparative study of new and traditional designs of a hammer mill. *Transactions of the ASABE*, 58(3), 585-596. <https://doi.org/10.13031/trans.58.10691>
- [3] Cao Liying, Zhang Yuepeng, Zhang Yubao et al. (2016). Influence of screen parameters optimization on screening efficiency of feed hammer mill. *Transactions of the Chinese Society of Agricultural Engineering*, 32(22), 284-288. <https://doi.org/10.11975/j.issn.1002-6819.2016.22.039>
- [4] Chen Junyu, Liu Bao, Li Pengfei. (2017). Study on motion state of mill hammer based on clearance joint. *Modern Machinery*, (4), 55-59. <https://doi.org/CNKI:CDMD:2.1018.960617>
- [5] Wang Di, He Changbin, Tian Haiqing, et al. (2020). Parameter optimization and experimental research on the hammer mill. *INMATEH Agricultural Engineering*, 62 (03): 341-350. <https://doi.org/10.35633/inmateh-62-36>
- [6] Wang Di, He Changbin, Wang Haiqing, et al. (2020). Design and experimental optimization of air oil triangle level for hammer mill. *INMATEH Agricultural Engineering*, 61 (02): 315-322. <https://doi.org/10.35633/inmateh-61-34>
- [7] Du Jianan, (2015). *Design and experimental research on wing shaped screen of hammer grinder*, MSc dissertation, Inner Mongolia Agricultural University, Hohhot/China
- [8] Li Xiuqing, (2021). *Simulation of corn grinding process of hammer mill and experimental study of hammer performance based on discrete element method*, MSc dissertation, Inner Mongolia Agricultural University, Hohhot/China
- [9] Li Zhen, Wei Anning, Cao Liying et al. (2019). Experimental research and optimal design of new feed hammer grinder's smashing performance. *Feed Industry*, 40(5), 6-10. <https://doi.org/10.13302/j.cnki.fi.2019.05.002>
- [10] Liu Weigang, (2019). *Analysis of straw grinding characteristics and optimization of grinding equipment*, MSc dissertation, Guizhou University, Guizhou/China
- [11] Ma Qian, Liu Fei, Zhao Manquan, (2016). Analysis of grinding Mechanism and Optimization of Hammer Structure of a grinder. *Journal of Agricultural Engineering*, 32 (Supplement 2): 7-15. <https://doi.org/10.11975/j.issn.1002-6819.2016.z2.002>
- [12] Mugabi, R., Eskridge, K. M., Weller, C. L. (2017). Comparison of experimental designs used to study variables during hammer milling of corn bran. *Transactions of the ASABE*, 60(2), 537-544. <https://doi.org/10.13031/trans.11656>
- [13] Qian Yi, Wang Di, Zhang Jue, et al. (2020). Numerical simulation and experimental research on the airflow field of the irregular screen of a grinder. *Journal of China Agricultural University*, 25 (03): 79-87. <https://doi.org/10.11841/j.issn.1007-4333.2020.03.10>
- [14] Qian Yi, (2021). *Optimization design and experimental research on the rotor structure of hammer grinder*, MSc dissertation, Inner Mongolia Agricultural University, Hohhot/China
- [15] Su Congyi, Wang Yongchang, Yu Xinguo et al. (2016). Cutting edge hammer blade is a new way to improve the efficiency of grinder. *Feed Industry*, 2016, 37 (01): 12-18. <https://doi.org/10.13302/j.cnki.fi.2016.01.003>
- [16] Xu Wei, Cao Chunping, Sun Yu. (2021). Optimization design of hammer structure parameters of hammer mill. *Journal of Agricultural Mechanization Research*, 43(1), 27-33. <https://doi.org/10.13427/j.cnki.njyi.2021.01.006>
- [17] ***China Agricultural Machinery Standardization Technical Committee, (2007), *Technical specification of quality evaluation for grinders, NY/T1554-2007*, Standards Press of China, Beijing/China.
- [18] ***China Agricultural Machinery Standardization Technical Committee, (2007), *Test method for feed mill, GB/T6971-2007*, Standards Press of China, Beijing/China.